Experimental investigation of the adhesive layer's impact on the Riv-Bonding process and joint quality

Yunpeng Liu[a], Li Han[b], Huan Zhao[a] and Xianping Liu[a,*]

[a] School of Engineering, University of Warwick, Coventry CV4 7AL, UK

[b] Hansher Consulting Ltd., Coventry, UK

* X.Liu@warwick.ac.uk

Abstract:

Interrupted experimental tests were carried out to investigate the impacts of adhesive layer on the Riv(et)-Bonding processes with different die types. The adhesive layer's influences on the quality of Riv-Bonded joints with different top sheet thickness (T_t) were also studied. It was found that the distribution of trapped adhesive was significantly affected by the T_t rather than by the die type. Deformation and fracture behaviours of top sheet were apparently influenced by the trapped adhesive. The adhesive layer negatively affected the interlock formation, while its effects on the remaining bottom sheet thickness depended heavily on the T_t.

Keywords: Self-piercing riveting; Riv-Bonded joint; Adhesive distribution; Joint quality; Die type; Top sheet thickness.

1 Introduction

Riv(et)-Bonding technique, which combines the advantages of adhesive bonding and self-pierce riveting (SPR), has been widely used in the automotive industry for the assembly of aluminium alloy car Body in White (BIW) structures [1]. The adhesive layer can effectively avoid the galvanic corrosion of SPR joints with different metal parts, and improve the noise, vibration and harshness (NVH) performance of the riveted structure. By simply involving an adhesive layer, the mechanical performance of the SPR joint could be significantly improved, including the static strengths [2] and the fatigue life [3]. In addition to the SPR technique, other mechanical fastening methods (e.g. clinching [4], electromagnetic riveting (EMR) [5] and bolting [6]) can also be combined with the adhesive bonding to enhance their mechanical performances. **Fig. 1** schematically shows the major steps

during the Riv-Bonding process. First, the adhesive is applied on the bottom sheet and distributed at the interface between the two sheets after the clamping process. Then, the punch moves downward and presses the rivet into the two sheets. Finally, all the tools are released and a Riv-Bonded joint is formed.

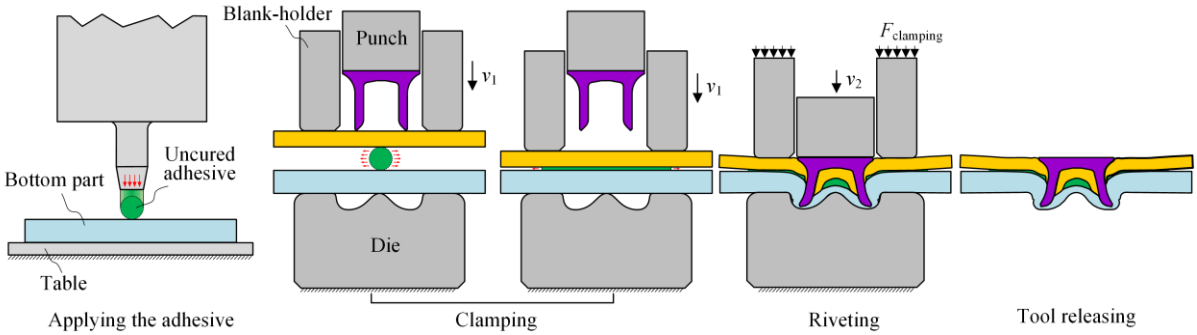

Fig. 1 Schematic of the Riv-Bonding process

In the past few decades, SPR technique has attracted a lot of attentions from the industrial and academic sectors. A large number of experimental and numerical studies have been carried out to expand its application ranges and to improve the joint mechanical performances. According to the research objectives, these studies can be divided into two groups. The first group focused on investigations of the joining process and the final joint quality, such as the deformation behaviours of the rivet and sheets, the changing trends of the interlock and the remaining bottom sheet thickness. For example, Haque et al. [7] experimentally found that, in addition to the joining process monitoring, the load-displacement curve can also be used to identify the events happened during the SPR process, such as the top sheet separation and the starting point of the rivet shank flare. Abe et al. [8] numerically explored the rivet flare behaviour and interlock formation with a two-dimensional (2D) simulation model in LS-DYNA. Ma et al. [9] experimentally investigated the effects of the rivet and die parameters on the rivetability of the AA6061-T6 and mild steel CR4 sheets. Hoang et al. [10] explored the possibility of joining aluminium alloy 6060 sheets with aluminium rivets. The second group paid more attention to the evaluations of the joint mechanical performances, such as the static strengths and fatigue life. For instance, Rao et al. [11] studied the failure modes and fatigue strength of the SPR joints with the carbon fibre reinforced polymer (CFRP) top sheet and the AA6111 bottom sheet under different loading conditions. Zhang et al. [12] evaluated the shear strength and fatigue life of SPR joints with 1420 aluminium–lithium alloy sheets. Huang et al. [13] developed a 3D simulation model using ABAQUS to predict the crack initiation, crack growth and the final fatigue life of SPR joints with aluminium alloy 6111-T4 sheets. Li et al. [14] and He et al. [15] systematically reviewed the numerical and experimental studies relating to the SPR technique. In addition, to improve the mechanical performances of connected joints, the traditional SPR process was also upgraded by some researchers, such as the friction self-piercing riveting (F-SPR) [16], the electromagnetic self-piercing riveting (E-SPR) [17,18] and the pre-holed self-piercing riveting

(PH-SPR) [19]. In fact, the joint mechanical strengths are directly linked with the magnitudes of the joint quality indicators, especially the interlock. Therefore, the investigations of SPR process lay a foundation for the optimization of SPR joint designs, and for the joint performance evaluation.

Riv-Bonding is developed from the SPR technique by adding a thin adhesive layer between the connected sheets. This additional bonded connection effectively improves the joint mechanical strengths and advances the NVH performance of the connected structures. Therefore, the Riv-Bonding technique has been widely applied in the automotive industry. However, in the public domain, there is still a limited amount of literature relevant to the Riv-Bonding technique. Most of the accessible studies focused mainly on the performance evaluation of Riv-Bonded joints rather than the Riv-Bonding process. Baurova et al. [20] found that the Riv-Bonded joints with a hot-melt adhesive had apparently higher shear strengths compared to the SPR joints. He et al. [21] investigated the shear strength and energy absorption of the Riv-Bonded joints made with AA5754 sheets and a 0.1mm adhesive layer. Liu and Zhuang [22] experimentally studied the mechanical strengths and failure mechanisms of the Riv-Bonded joints with the CFRP top sheet and the AA5754-H22 bottom sheet. Sun et al. [3] found that the application of the adhesive Dow Betamate 4601 significantly enhanced the fatigue strength of the SPR joints under the lap-shear loading condition, but a smaller improvement was observed under the cross-tension loading condition. Miyashita et al. [2] studied the shear strength and fatigue strength of the Riv-Bonded joints with AM50 magnesium alloy sheets. Presse et al. [23] developed a simulation model of Riv-Bonded joints with aluminium EN AW-6016 and high strength steel CR330Y590T-DP sheets, and successfully predicted the joint fatigue life by superposing the contributions of the riveted connection and the bonded connection. Wu et al. [1] experimentally studied the fatigue failure behaviour of Riv-Bonded joints with AA6111-T4 sheets and a toughened epoxy adhesive (i.e. BETAMATE 4601^{TM}), and proposed a mechanism-based fatigue life evaluation method for the Riv-Bonded joints. Actually, the performance of the Riv-Bonded joint depends on both the bonded connection and the riveted connection. The above studies emphasize the benefits of the adhesive layer on the overall joint performance, but rarely mention the effects of the adhesive layer on the riveted connection. Few reports relevant to the impact of adhesive layer on the joining process and the joint quality can be found in the public domain.

For a specific joint configuration, the viscosity and the application amount of the adhesive may significantly influence the rivet and sheet deformations, and thus alter the quality of the riveted connection. With the same type of adhesive and application amount, changes of the joint configurations (e.g. the sheet thickness, sheet material and the die type) may also alter the effects of the adhesive layer on the riveted connection. Fricke and Vallée [24] found that a larger amount of adhesive was trapped around the joining region in Riv-Bonded joints with the steel

HC340LA sheets. Hahn and Wibbeke [25] mentioned that the adhesive layer would impose limited influences on the quality of the riveted connection when the total sheet thickness was greater than 2.0mm, but obvious influences when the sheet thickness was smaller than 1.6mm. Test results from the study of Moroni [26] strongly supported this view: no adhesive was found around the joining region of the Riv-Bonded joints with 2.0mm/2.0mm AA5754-H32 sheets. In addition, the flow behaviour of the uncured adhesive is sensitive to the strain rate [24], and therefore the riveting speed may also affect the quality of the Riv-Bonded joints. There is still a lot of work to do in order to have a comprehensive understanding of the Riv-Bonding process.

This study aims to explore the influences of the adhesive layer on the joining process, including the deformations of the rivet and sheets, the changes of the riveting force and the adhesive distribution. The interrupted experimental tests were carried out to visually observe the joint formation during the Riv-Bonding process. Two types of die (i.e. Flat die and Pip die) were utilized to investigate the effects of die type on the Riv-Bonding processes. The potential defects and benefits induced by the adhesive layer on the riveted connection with different dies were also identified and analysed. Moreover, the influences of the adhesive layer on the quality of the riveted connection were evaluated. The influences of top sheet thickness on the adhesive distribution and joint quality were also studied.

2 Experimental procedures

2.1 Materials

In this study, the boron steel semi-tubular rivet with the hardness 280±30HV10 was adopted in all joints. Its nominal dimensions are shown in **Fig. 2**. The material for both top and bottom sheets is aluminium alloy AA5754. The structure adhesive SikaPower 498, which is widely used in the automotive industry, was selected for the Riv-Bonded joints. It is a one component epoxy resin-based adhesive, and very suitable for oiled and coated surfaces [27]. **Table 1** lists the basic properties of this adhesive.

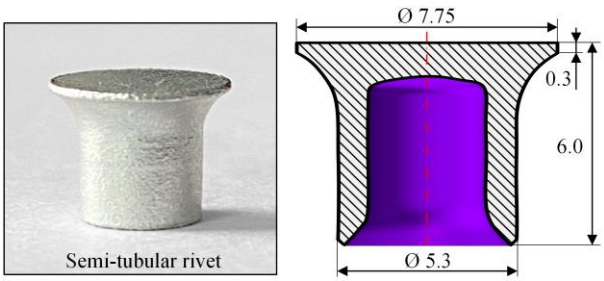

Fig. 2 Schematic of the semi-tubular rivet (in mm)

Table 1 Properties of the adhesive SikaPower 498 [27]

Name	Dynamic viscosity (Pa·s)		Application temperature (℃)	Curing time (min)	Elongation (After curing)
	(25℃)	(55℃)			
SikaPower 498	Approx. 3000	Approx. 1300	50~60	20 (175℃)	5.0%

2.2 Experiment plan

To study the influences of the adhesive layer on the riveting process, as listed in **Table 2**, interrupted experimental tests of the SPR process and the Riv-Bonding process were carried out. The top sheet thickness (T_t) and the bottom sheet thickness (T_b) are fixed at 1.2mm and 2.0mm respectively. Two types of die (i.e. Pip die and Flat die) presented in **Fig. 3** were adopted to explore the impact of the die type on the joining process. Each riveting process was interrupted at five different positions as shown in **Fig. 4**. This was achieved by controlling the predefined magnitude of final rivet head height (H_1) in the SPR system. In addition, as listed in **Table 3**, the influences of the T_t on the Riv-Bonded joint quality and the adhesive distribution were also investigated experimentally. Twelve joint configurations with or without the adhesive layer were made using two different dies, and three levels of the T_t were chosen.

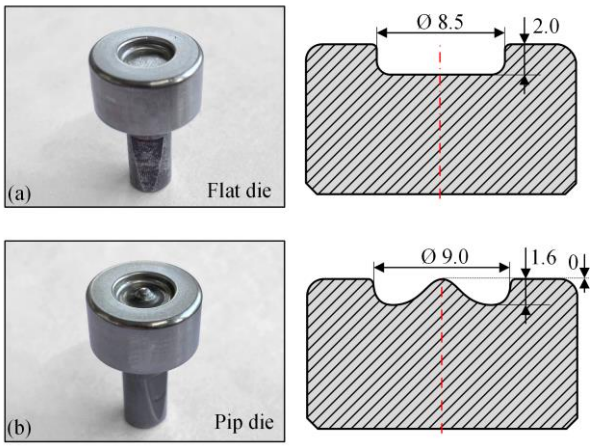

Fig. 3 Schematic of the (a) Flat die and (b) Pip die (in mm)

Table 2 Interruption tests of SPR process and Riv-Bonding process with different die types

Joint no.	Thickness (mm)		Adhesive SikaPower 498	Rivet head height/H_1 (mm)	Rivet (Boron steel)	Die type
	Top sheet/T_t (AA5754)	Bottom sheet/T_b (AA5754)				
P1-1	1.2	2.0	--	4.0	C5.3*6.0 (280±30HV10)	Pip die
P1-2				3.0		
P1-3				2.0		
P1-4				1.0		
P1-5				0.0		
P2-1	1.2	2.0	Yes (Ø3.0mm nozzle)	4.0		
P2-2				3.0		
P2-3				2.0		
P2-4				1.0		

P2-5				0.0		
F1-1				4.0		
F1-2				3.0		
F1-3	1.2	2.0	--	2.0		
F1-4				1.0		
F1-5				0.0	C5.3*6.0 (280±30HV10)	Flat die
F2-1				4.0		
F2-2			Yes (Ø3.0mm nozzle)	3.0		
F2-3	1.2	2.0		2.0		
F2-4				1.0		
F2-5				0.0		

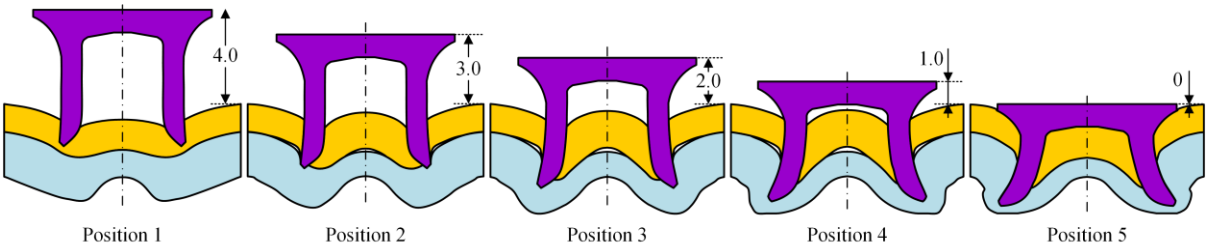

Fig. 4 Schematic of five positions during the interrupted experimental tests of SPR process and Riv-Bonding process

Table 3 SPR and Riv-Bonded joints with different top sheet thicknesses (T_t)

Joint no.	Thickness (mm)		Adhesive SikaPower 498	Rivet (Boron steel)	Die type
	Top sheet/T_t (AA5754)	Bottom sheet/T_b (AA5754)			
P3-1	1.2				
P3-2	1.8		--		
P3-3	2.5	2.0		C5.3*6.0 (280±30HV10)	Pip die
P4-1	1.2		Yes (Ø3.0mm nozzle)		
P4-2	1.8				
P4-3	2.5				
F3-1	1.2				
F3-2	1.8		--		
F3-3	2.5	2.0		C5.3*6.0 (280±30HV10)	Flat die
F4-1	1.2		Yes (Ø3.0mm nozzle)		
F4-2	1.8				
F4-3	2.5				

2.3 Sample preparation

The specimen size of the SPR and Riv-Bonded joints is 40mm×40mm as presented in **Fig. 5**. All the rivets, dies and adhesive were provided by the Tucker GmbH, whilst the AA5754 sheets were provided by Jaguar Land Rover (JLR). To reflect the practical application conditions used in the automotive industry, the rivet and sheets were directly used without any surface treatment (e.g. Degreasing). The adhesive was preheated to about 55℃ to reduce its viscosity, and then applied on the bottom sheet along the centre line with a cartridge gun, as shown in **Fig. 6**. This is because the adhesive SikaPower 498 has a poor fluidity at the ambient temperature due to the high viscosity (Approx. 3000Pa.s at 25℃ in **Fig. 7**). The amount of adhesive was controlled by a constant gun nozzle diameter

(i.e. 3.0mm), which also directly reflected the practical application conditions. Once the adhesive was applied on the bottom sheet, the top sheet was placed on the top of the adhesive. Then, the riveting process was carried out within a very short time to eliminate the temperature effect on the adhesive flow behaviour.

All the joints were made using the servo SPR system manufactured by Tucker GmbH, as shown in **Fig. 8**. The riveting speed was set to 300mm/s and the clamping force on the blank-holder was around 6.0kN controlled by a compressed spring. To ensure the effectiveness of the experiment results, three repeats for each joint configuration were performed. The Riv-Bonded joints were placed in a preheated oven at 175℃ for 20mins to cure the adhesive layer. To eliminate the influences of the heat treatment on the joint quality, the corresponding SPR joints were also heat treated under the same conditions.

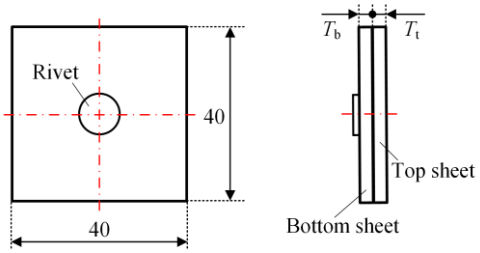

Fig. 5 Specimen dimensions of the SPR and Riv-Bonded joints (in mm)

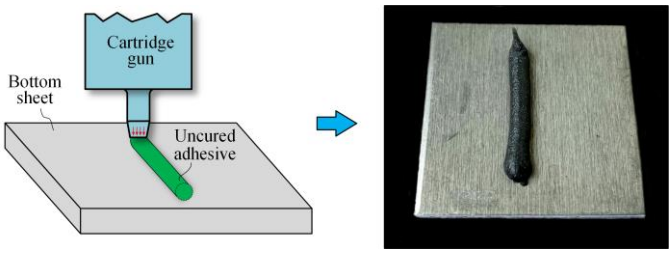

Fig. 6 Schematic of applying the uncured adhesive on the bottom sheet

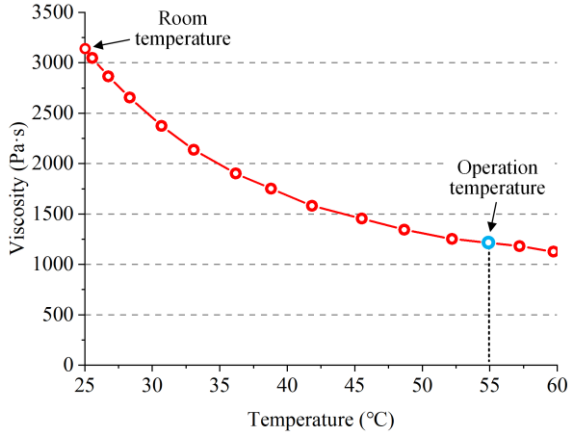

Fig. 7 Dynamic viscosity-temperature curve of the adhesive SikaPower 498 [27]

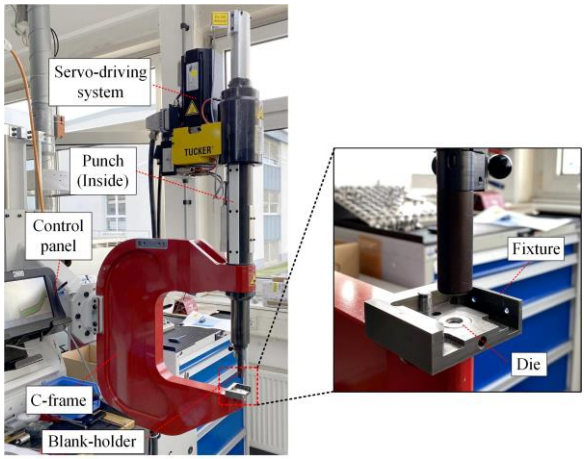

Fig. 8 Structure of the Tucker SPR system

2.4 Geometrical characterization of the SPR and Riv-Bonded joints

All the joints were sectioned using an abrasive-wheel cutting machine. According to the [28], any improper cutting position will impose apparent influences on the observed joint cross-sectional profile, and the measured magnitudes of joint quality indicators. Therefore, to ensure the cross-sectional profile on the joint centre plane was captured, the joint was cut at a position slightly offsetting the joint central plane as shown in **Fig. 9** with a specially designed fixture. This preserved enough space for the subsequent surface polishing work. The joint cross-sectional profile was inspected with an optical microscope after polishing, as shown in **Fig. 10**. The rivet head height (H_1), the interlock (I_1), the remaining bottom sheet thickness under the rivet tip (t_{tip}) and at the joint centre (t_c) were measured to evaluate the quality of the riveted connection for the SPR and Riv-Bonded joints. The radius of the interlock inner boundary (R_{in}) and outer boundary (R_{out}) were measured to analyse the interlock formation as well as the rivet shank flare behaviour. Meanwhile, the adhesive distribution within the Riv-Bonded joints was also inspected visually.

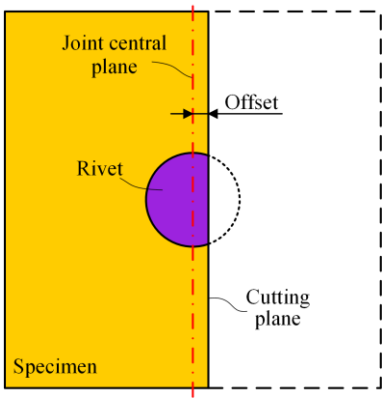

Fig. 9 Schematic of the specimen cutting position

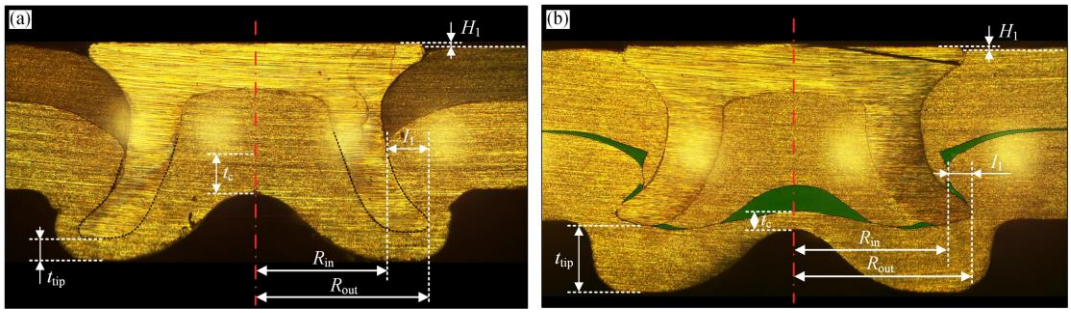

Fig. 10 Dimensions measured on the cross-sectional profiles of (a) the SPR joint and (b) the Riv-Bonded joint

3 Results and discussion

3.1 Influence of the adhesive layer on the joining process

Using the interrupted experimental tests, the joint cross-sectional profiles at five positions during the SPR process and the Riv-Bonding process with two types of die were extracted and compared in **Fig. 11** and **Fig. 12** respectively. From the **Fig. 11**(b) and **Fig. 12**(b), it can be seen that a large amount of adhesive was trapped between the top and bottom sheets regardless of the die type. The preheated adhesive (approx. 55°C) had a high flowability and thus applied a uniform hydraulic pressure on the top and bottom sheets. This changed the initial interactive forces between the two sheets in the SPR joints. As a result, the deformation behaviours of the rivet and sheets were affected. In the following sections, flow behaviour of the adhesive, deformation behaviours of the two sheets, flare behaviour of the rivet shank and variation of the riveting force were analysed in detail.

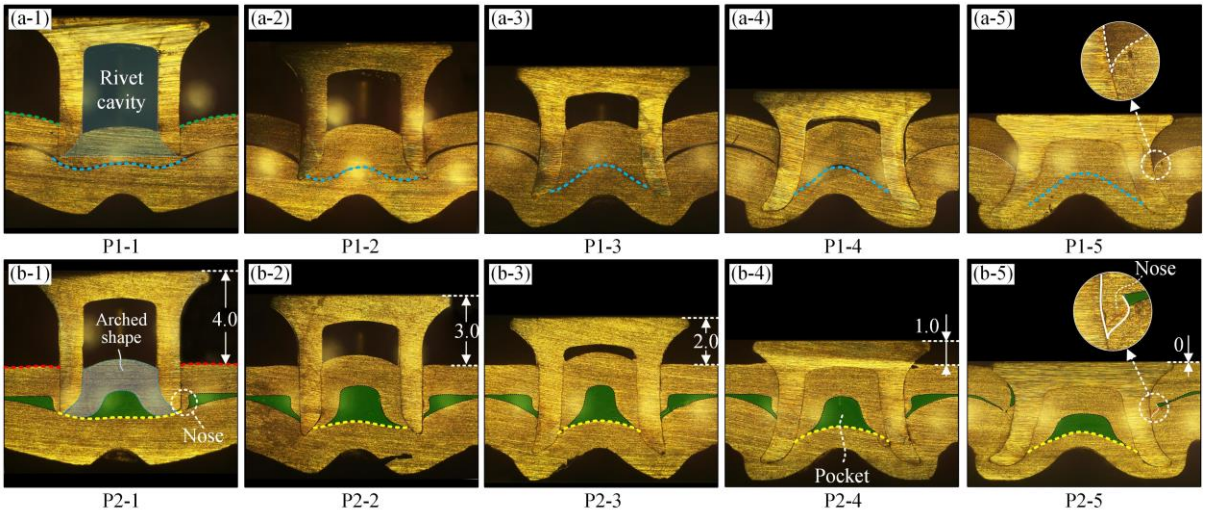

Fig. 11 Comparison of the joint cross-sectional profiles during the (a) SPR process and (b) Riv-Bonding process with the pip die

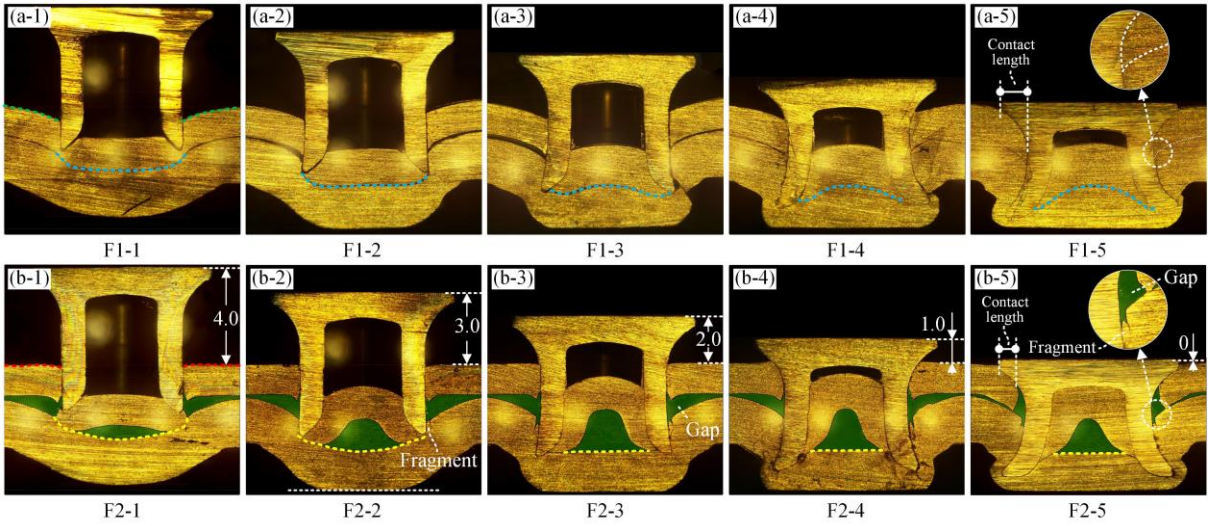

Fig. 12 Comparison of the joint cross-sectional profiles during the (a) SPR process and (b) Riv-Bonding process with the flat die

3.1.1 Flow behaviour of the adhesive layer

As shown in **Fig. 11**(b-1), after the top sheet was penetrated by the rivet, the remaining adhesive in the joining region was divided into two parts. A large part of the adhesive was trapped into the rivet cavity and the amount kept unchanged as the riveting process continued from **Fig. 11**(b-1) to **Fig. 11**(b-5). This large size adhesive pocket might be associated with the relatively low stiffness of the 1.2mm AA5754 top sheet and the low flowability of the adhesive SikaPower 498 (viscosity > 1300Pa·s) employed in this study. Another part of the adhesive was squeezed outside the rivet shank, and its total amount apparently reduced at the end of the joining process as shown in **Fig. 11**(b-5). Only a thin adhesive layer was left between the two sheets. This is because some adhesive was pressed out of the joining region due to the high pressure from the rivet head. With the flat die, a similar adhesive distribution was observed during the joining process in **Fig. 12**(b), and the only difference is that more adhesive was left outside the rivet shank at the end of the riveting process. This is because a gap was formed between the rivet shank and the top sheet as shown in **Fig. 12**(b-5). The main reason for this difference is that the top sheets underwent different separation/fracture behaviours with the pip die and the flat die. Detailed explanations about the different top sheet fracture behaviours were given in the next section.

During the Riv-Bonding process, the movement of the blank-holder may impose a significant influence on the initial amount of adhesive trapped in the joining region. Compared with the aluminium alloy AA5754 sheets, the uncured adhesive is much easier to be deformed. As shown in **Fig. 13**(a), the uncured adhesive more likely distributes evenly between the two sheets with a low blank-holder speed. Because there is enough time for the adhesive around the joint centre to flow outward. In contrast, with a high blank-holder speed, the uncured adhesive more likely distributes unevenly at the interface of the two sheets as shown in **Fig. 13**(b). This is because the

adhesive around the joint central area does not have enough time to escape through the narrow gap under the blank-holder. The high sensitivity of the adhesive flow behaviour to the strain rate [29] might also contribute to these different initial adhesive distributions. To reflect the practical application conditions used in the automotive industry for car body assembly, a relatively high blank-holder speed (i.e 100mm/s) and a high clamping force (approx. 6.0kN) were utilized throughout the experimental tests in this study. The high blank-holder speed is aimed at improving the joining efficiency by shortening the manufacturing cycle time spend on each Riv-Bonded joint. The high clamping force is designed to restrict the relative movements between the sheets during the riveting process. When the blank-holder moved rapidly downward and struck on the two sheets, the strong impact mainly applied on the circle region underneath the blank-holder. As a result, the adhesive around this region was squeezed partially towards the joint centre and partially outside the joining region. **Fig. 14** shows the adhesive distribution in the Riv-Bonded joint F2-1. It can be seen that only a very thin adhesive layer was left around the clamping region, but a large amount adhesive was trapped in the joining region. The constant clamping force (Approx. 6.0kN) was then applied on the blank-holder. This not only restricted the relative movements of the two sheets, but also limited the outward flow of the adhesive trapped in the joining region. Therefore, the blank-holder speed and the magnitude of clamping force should be selected carefully when fabricating the Riv-Bonded joints.

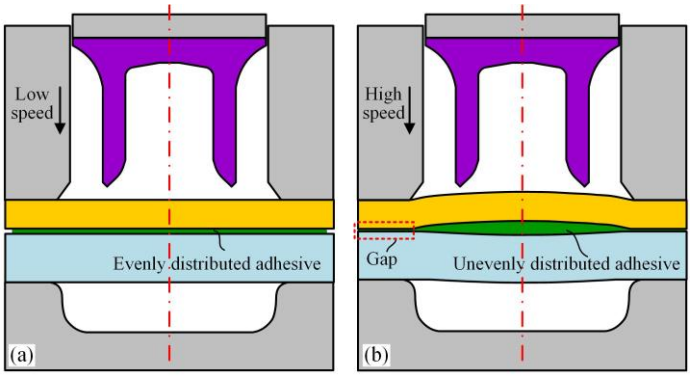

Fig. 13 Schematics of adhesive distribution after the clamping process with (a) a low blank-holder speed and (b) a high blank-holder speed

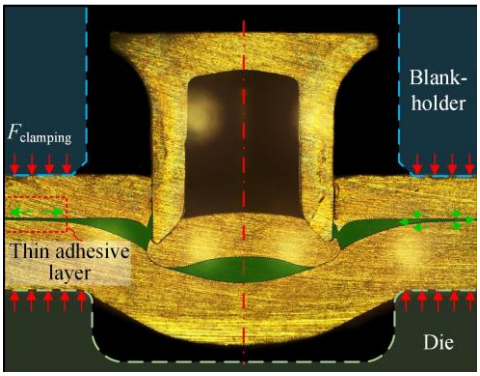

Fig. 14 Remaining adhesive around the clamping region between the blank-holder and the die (Joint F2-1)

3.1.2 Deformations of the top and bottom sheets

By comparing the cross-sectional profiles of SPR joints and Riv-Bonded joints in **Fig. 11** and **Fig. 12**, it can be found that the deformation behaviours of the top and bottom sheets were significantly affected by the adhesive layer. As shown in **Fig. 11**(a-1) and **Fig. 12**(a-1), the top sheet outside the rivet was bent downward (Green lines) when pierced by the rivet shank in the SPR joints. In contrast, as shown in **Fig. 11**(b-1) and **Fig. 12**(b-1), it still remained almost flat (Red lines) after the top sheet was penetrated in the Riv-bonded joints. Such different top sheet deformations were highly linked with the resistance force that the adhesive applied on the bottom surface of the top sheet outside the rivet. Due to the increasing forces imposed on the two sheets by the rivet and die, the hydraulic pressure in the trapped adhesive reached to a very high level. This effectively prevented the large downward movement of the top sheet in the Riv-Bonded joint. In practical applications, the top and bottom sheets sometimes cannot be tightly connected with the SPR technique if the top sheet undergoes a too large downward movement. For example, **Fig. 15** illustrates a SPR joint with a large gap formed between the rivet head and the top sheet. By adding an adhesive layer, the less downward movement of the top sheet outside the rivet may have a great possibility to avoid the formation of such gaps, and therefore effectively eliminate this kind of defect in the initial SPR joints.

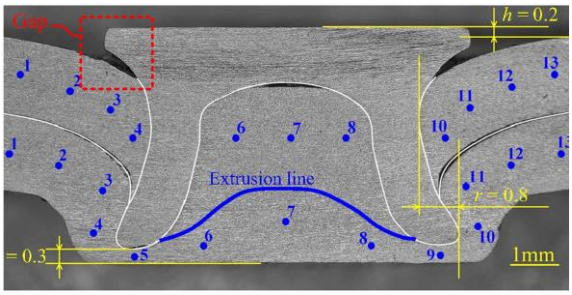

Fig. 15 A loosely connected SPR joint with a gap formed between the rivet head and the top sheet [30]

In addition to the deformation behaviour, the fracture behaviours of top sheets with the flat die and pip die were also affected by adding the adhesive layer. To facilitate the explanation, **Fig. 16** schematically plots the top sheet penetration processes of the Riv-Bonded joints with the flat die and pip die. As shown in **Fig. 16**(a-1) and (b-1), the trapped adhesive at the joint centre flowed outward (Yellow arrows) with the increment of the rivet displacement. The top sheet outside the rivet underwent less downward movement, but the top sheet underneath the rivet was pressed downward rapidly, as shown in **Fig. 16**(a-2) and (b-2). This induced an obvious displacement difference between the two parts of top sheet. With the pip die, the die pip applied an increasing resistance force on the bottom sheet, and thus the downward movements of the two sheets were effectively restricted as shown in **Fig. 16**(a). Due to the different displacements of the two parts of top sheet, the top sheet material around the rivet

tip was stretched and experienced a large plastic deformation as shown in **Fig. 16**(a-3). With further increment of the rivet displacement, the top sheet was gradually penetrated by the rivet shank and a ductile fracture was observed as shown in **Fig. 16**(a-4). A long nose was formed because of the severely localized top sheet deformation. However, due to the lack of die pip, the flat die could not provide a sufficient resistance force at the central area of the bottom sheet during the early stage of the joining process, as shown in **Fig. 16**(b-1). So the adhesive pocket, the top sheet underneath the rivet and the bottom sheet around the joining region were pressed downward rapidly by the rivet as shown in **Fig. 16**(b-2). With the increment of the rivet displacement, the riveting force gradually increased but the remaining top sheet thickness around the rivet tip decreased rapidly. After the top sheet thickness reduced to a threshold value, the stresses within the thinnest region surpassed the ultimate tensile strength of the top sheet material. As a result, initial formation of cracks started on the top sheet, and a premature fracture of the top sheet occurred as the cracks propagated in **Fig. 16**(b-3). The insufficient resistance from the bottom sheet, which allowed the rapid downward movement of the top sheet underneath the rivet, significantly contributed to this early top sheet separation. This type of fracture behaviour was also reported in [14] with a very deep flat die as shown in **Fig. 17**(a). Due to the premature failure of top sheet, fragments were formed with further increment of the rivet displacement as shown in **Fig. 16**(b-4). This type of fragments was also reported in [31] with a low ductile top sheet as shown in **Fig. 17**(b). Furthermore, because of the premature top sheet fracture with the flat die, a gap was formed between the top sheet and the rivet shank as shown in **Fig. 12**(b-5). On the one hand, this may weaken the riveted connection due to the smaller contact length between the rivet head and the top sheet in **Fig. 12**(b-5) than in **Fig. 12**(a-5). On the other hand, the adhesive accumulated in this gap could bond the rivet and the top sheet together once cured. This might affect the total connection strength of the Riv-Bonded joint to some degree, and more efforts are required to disclose its effects using experimental or numerical approaches.

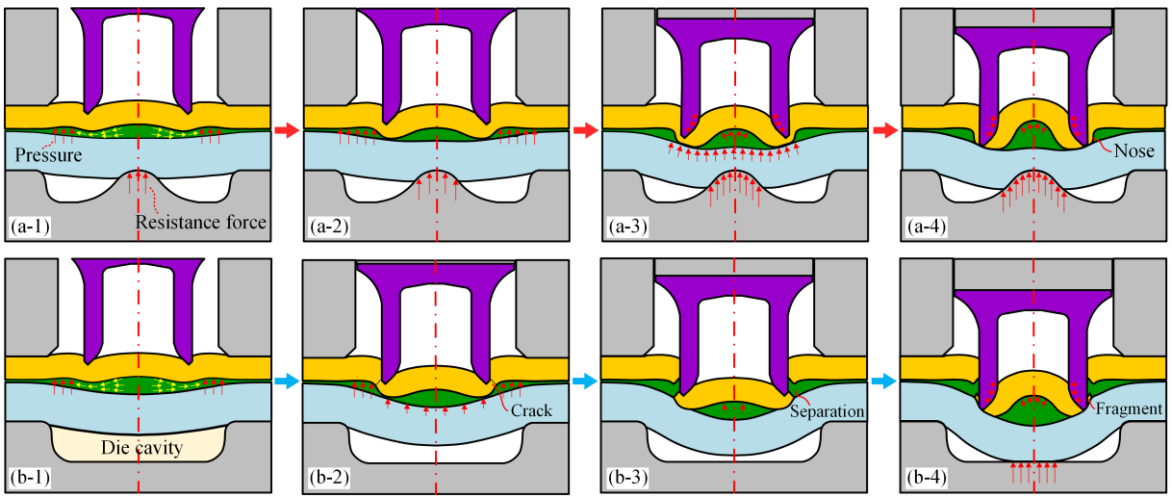

Fig. 16 Schematic of the top sheet penetration processes in Riv-Bonded joints with (a) the pip die and (b) with the flat die

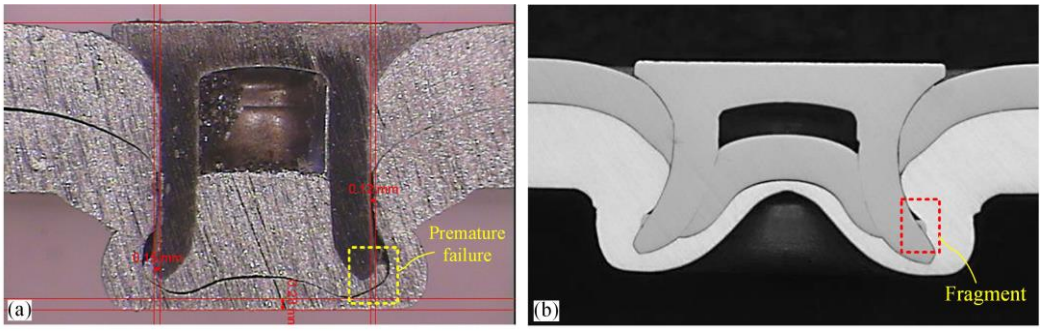

Fig. 17 Joint cross-sectional profiles with (a) premature failure of top sheet [14] and (b) top sheet fragment [31]

The changes of the top sheet fracture behaviour after adding the adhesive layer also bring some influences on the interlock formation. With the pip die, the long nose formed on the top sheet was partially pressed into the interface between the rivet shank and the bottom sheet, as shown in **Fig. 11**(b-5). While with the flat die, the top sheet fragments were pressed downward and trapped into the interface between the rivet shank and the bottom sheet in **Fig. 12**(b-5). From the definition of interlock, both of the inserted nose and the trapped fragments will impose negative effects on the formation of interlock, and therefore may weaken the mechanical strengths of the riveted connection.

From the **Fig. 11** and **Fig. 12**, it can also be seen that, regardless of the die types, the top sheet underneath the rivet underwent a larger plastic deformation in the Riv-Bonded joints than in the corresponding SPR joints. However, slightly different deformation behaviours of this part of top sheet were observed during the Riv-Bonding process with different types of dies. With the pip die, as shown in **Fig. 11**(b-1), the top sheet underneath the rivet was already deformed to an arched shape at the moment when the top sheet was penetrated. In contrast, with the flat die, this part of top sheet only slightly bended upward as shown in **Fig. 12**(b-1). This is because the die pip prevented the rapid downward movement of the sheets, and the hydraulic pressure within the trapped adhesive increased with the increment of the rivet displacement. A large hydraulic force was applied at the central area of the top sheet, and led to the rapid deformation of the top sheet underneath the rivet. For Riv-Bonded joints with the flat die, rapid deformation of this part of top sheet occurred after the bottom sheet contacted the bottom of the die cavity in **Fig. 12**(b-2). This is because the hydraulic pressure in the adhesive pocket could only increase after the bottom sheet stopped the rapid downward movement by reaching the bottom of the die cavity. Therefore, the rapid deformation of the top sheet underneath the rivet happened apparently later in the Riv-Bonded joints with the flat die than with the pip die. The following deformation behaviour of this top sheet part was quite similar in the Riv-Bonding processes with the pip die and the flat die. It is also worth mentioning that, due to the trapped adhesive pocket, the rivet cavity was filled at a faster speed in the Riv-Bonded joints than in the corresponding

SPR joints. According to [32], this change may affect the riveting force and the bottom sheet thickness distribution. These influences will be discussed in the following sections.

The deformation behaviour of the bottom sheet was also affected by the involved adhesive layer. With the pip die, at the same rivet head height (H_1), the curvature of the top surface on the bottom sheet was always smaller in the Riv-Bonded joints than in the SPR joints as shown in **Fig. 11**. In contrast, with the flat die, the trapped adhesive pocket led to a larger curvature of the bottom sheet before the bottom sheet contacted the bottom of the die cavity, as shown in **Fig. 12**(a-1) and **Fig. 12**(b-1). While the bottom sheet around the joint centre gradually became flat again in **Fig. 12**(b-2)~(b-5) after the bottom sheet contacted the bottom of the die cavity. This is mainly attributed to the rapid deformation of the top sheet underneath the rivet and the uniform hydraulic pressure applied on the bottom sheet.

3.1.3 Flare behaviour of the rivet shank

Due to the changes of the top and bottom sheet deformations, the rivet shank flare behaviour in the Riv-Bonded joints also became slightly different from that in the corresponding SPR joints. **Fig. 18** shows the variation curves of the deformed rivet shank diameter (D_1=2R_{out}) during the joining processes with or without the adhesive layer. A similar increasing pattern of the D_1 was found on the four curves: it firstly increased slowly at the early stage of the joining processes and then sharply increased. Close to the end of the joining processes, the D_1 increased almost linearly with the decline of the rivet head height (H_1), which agreed well with the results reported by Haque et al. [33]. According to the different increasing speeds, each variation curve of the D_1 can be roughly divided into a slow increment phase and a rapid increment phase.

By comparing the changing curves with or without the adhesive layer, it was found that the starting point of the rapid increment phase was altered after adding the adhesive layer. As shown in Zone 1 of **Fig. 18**(a), the rapid increment of the D_1 with the pip die was delayed from the Point *A* in the SPR joint P1-5 to the Point *B* in the Riv-Bonded joint P2-5. Similarly, as shown in Zone 2 of **Fig. 18**(b), the rapid rivet shank flare with the flat die was also slightly delayed in the Riv-Bonded joint F2-5 compared with that in the SPR joint F1-5. According to the results reported in [32], the rapid rivet shank flare started after the die cavity space underneath the rivet was fully filled. Therefore, the changes of rivet shank flare behaviour before and after adding the adhesive layer can be explained from the view of die cavity filling conditions. The threshold filling conditions of the pip die (Region 1) and the flat die (Region 2) for the rapid rivet shank flare are shown in **Fig. 19**(a) and **Fig. 19**(b) respectively. It can be seen that, due to the existence of die pip, the volume of the Region 1 in the pip die is obvious smaller than

that of the Region 2 in the flat die. So the Region 1 is much easier to be filled up than the Region 2. As a result, the rapid increment of the D_1 started earlier with the pip die than with the flat die as shown in **Fig. 18**. This phenomenon also indicated the contribution of the die pip to the rivet shank flare. As shown in **Fig. 19**(c), with the pip die, the Region 1 in the SPR joint was nearly filled up at H_1=4.0mm, but was just fully filled at H_1=3.0mm in the corresponding Riv-Bonded joint. This is because the large hydraulic pressure within the trapped adhesive pocket caused a larger deformation of the top sheet underneath the rivet, and thus delayed the filling of the Region 1 in the Riv-Bonded joint. Similarly, with the flat die, the Region 2 was completely filled up in the SPR joint and was nearly filled up in the Riv-Bonded joint at H_1=3.0mm as shown in **Fig. 19**(d). The trapped adhesive pocket with the flat die also caused a larger deformation of the top sheet underneath the rivet. This is attributed to the great hydraulic pressure within the trapped adhesive pocket. However, the trapped adhesive did not apparently affect the downward movement of the bottom sheet material around the joining region, and thus imposed limited influence on the filling of the Region 2 in the Riv-Bonded joint. The filling condition changes of the Region 1 and Region 2 in **Fig. 19** clearly explained the delay of the rapid increment phase after adding the adhesive layer in **Fig. 18**.

During the rapid increment phase, with either the pip die or the flat die, the increment speeds of the D_1 before and after adding the adhesive layer were nearly constant and very close to each other as shown in **Fig. 18**. At the end of the joining processes, the maximum values of the D_1 were a little bit smaller in the Riv-Bonded joints P2-5 and F2-5 compared with that in the SPR joints P1-5 and F1-5.

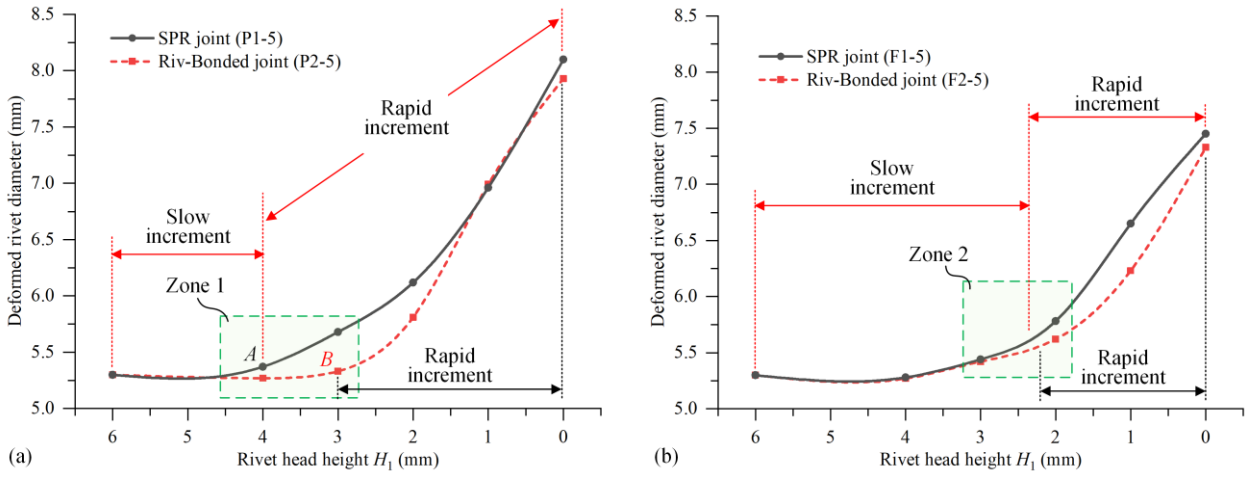

Fig. 18 Variation curves of the deformed rivet shank diameter (D_1) with or without the adhesive layer: (a) Pip die and (b) Flat die

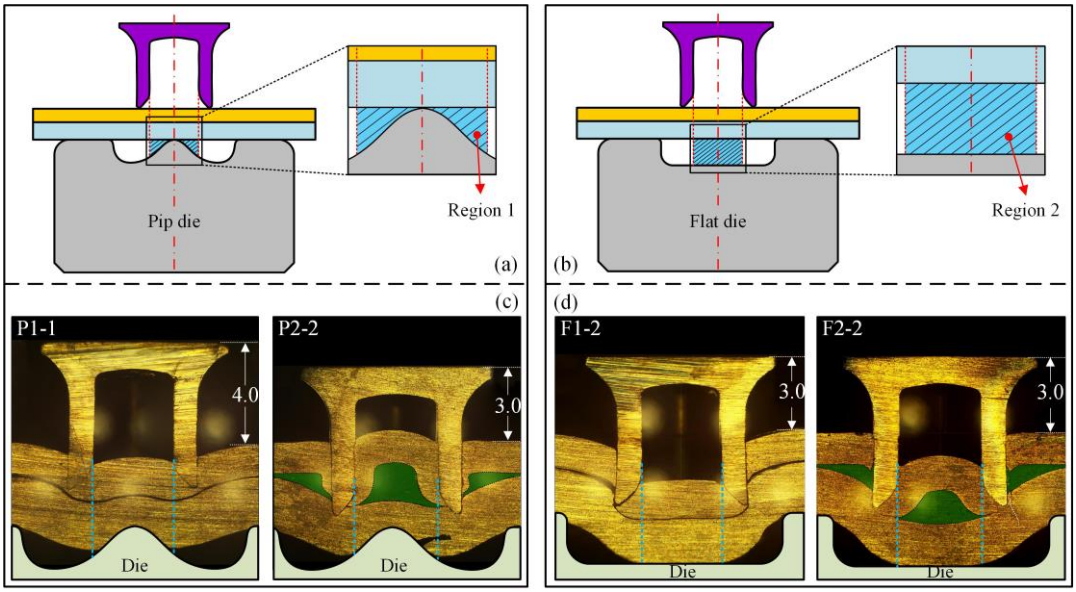

Fig. 19 Threshold filling conditions of the die cavity for rapid rivet shank flare with the pip die and flat die

3.1.4 Riveting forces

The load-displacement curves during the joining processes of the SPR joints P1-5, F1-5 and the Riv-Bonded joints P2-5 and F2-5 are given in **Fig. 20**. A similar changing trend of the riveting force was observed on the four curves: it first increased slowly at the early stage of the joining process and then increased rapidly at the end of the joining process. During the slow increment phase, the riveting force was slightly smaller in the Riv-Bonded joints P2-5 and F2-5 than that in the corresponding SPR joints P1-5 and F1-5. As shown in **Fig. 20**(a), the turning point between the slow increment and the rapid increment of riveting force was very clear, and appeared earlier in the Riv-Bonded joint P2-5 (Point B) than in the SPR joint P1-5 (Point A) with the pip die. This is because the rapid increment of the riveting force was directly caused by the fully filled rivet cavity. The trapped adhesive pocket speeded up the filling of the rivet cavity, and therefore led to the shift of the turning point from A to B. In contrast, as shown in **Fig. 20**(b), the turning point in the SPR joint F1-5 with the flat die (Point C) was not obvious. This is because the rivet cavity in this joint was not fully filled as shown in **Fig. 12**(a-5). After adding the adhesive layer, the rivet cavity in the Riv-Bonded joint F2-5 was filled up almost at the end of the joining process as shown in **Fig. 12**(b-4)(b-5). So the trapped adhesive did not impose obvious influences on the turning point (Point D) in the Riv-Bonded joint F2-5. During the rapid increment phase, the increasing speed of riveting force reduced to a smaller value in the Riv-Bonded joint P2-5 than in the SPR joint P1-5. This is because the rivet cavity in the Riv-Bonded joint P2-5 was partially filled with the uncured adhesive, which was much easier to be deformed than the sheet material and thus imposed less resistance on the rivet. While the rapid increment speed of the riveting force was almost the same in the SPR joint F1-5 and the Riv-Bonded joint F2-5. Finally, the maximum riveting force

in the Riv-Bonded joint P2-5 was approx. 4kN smaller than that in the SPR joint P1-5. The maximum riveting force in the Riv-Bonded joint F2-5 was approx. 3kN greater than that in the SPR joint F1-5. Therefore, the adhesive layer would not significantly affect the maximum riveting force required.

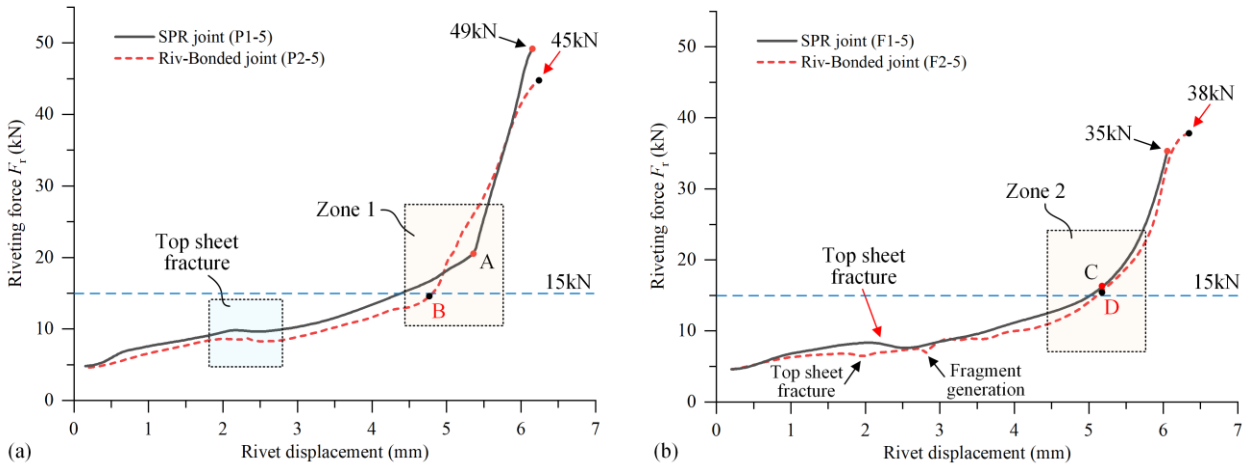

Fig. 20 Load-displacement curves during the joining processes with or without the adhesive layer (a) Pip die and (b) Flat die

3.2 Effects of the top sheet thickness (T_t) on the Riv-Bonded joint

According to [34], the flexural rigidity of the sheet (D) depends heavily on the sheet thickness (h) as shown in Eq.(1). The E and v denote the Young's modulus and the Poisson's ratio of the sheet material. Increment of the h would significantly increase the sheet flexural rigidity and thus makes the sheet more difficult to be deformed. **Fig. 21** and **Fig. 22** shows the joint cross-sectional profiles of the SPR and Riv-Bonded joints with 1.2mm, 1.8mm and 2.5mm top sheets. It can be seen that the top sheet thickness (T_t) not only influenced the flexural rigidity of the top sheet, but also directly affected the length of rivet shank inserted into the bottom sheet. As a result, the deformed shapes of the rivet and the sheets, the distribution of the trapped adhesive, and the magnitudes of joint quality indicators (i.e. interlock and the remaining bottom sheet thickness) were significantly influenced. These changes were analysed and discussed individually in the following sections.

$$D = \frac{Eh^3}{12\left(1-v^2\right)} \tag{1}$$

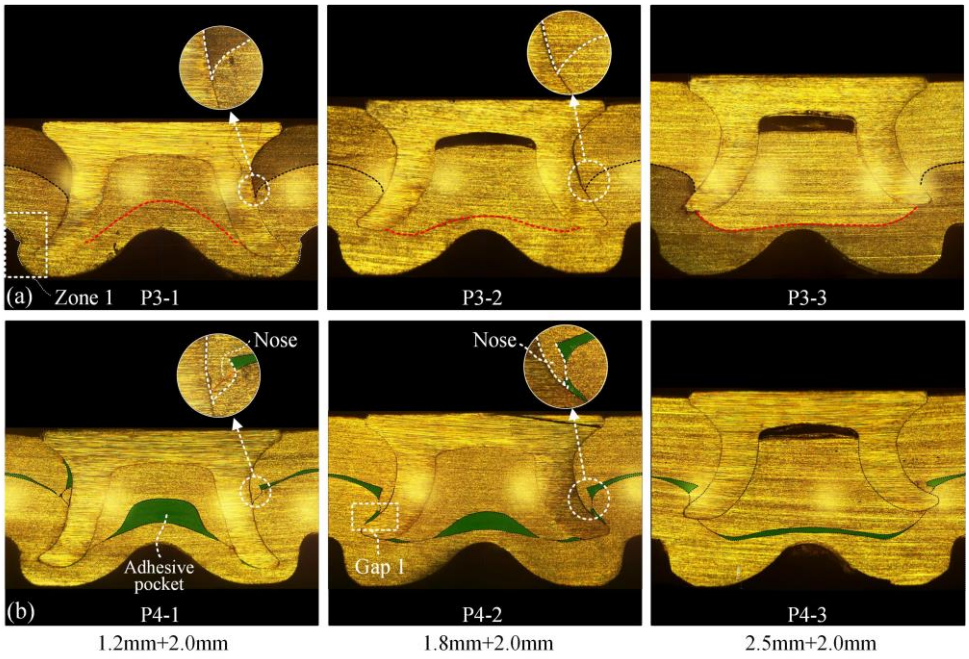

Fig. 21 Cross-sectional profiles of the SPR joints P3-1~P3-3 and the Riv-Bonded joints P4-1~P4-3 with different top sheet thicknesses T_t (Pip die)

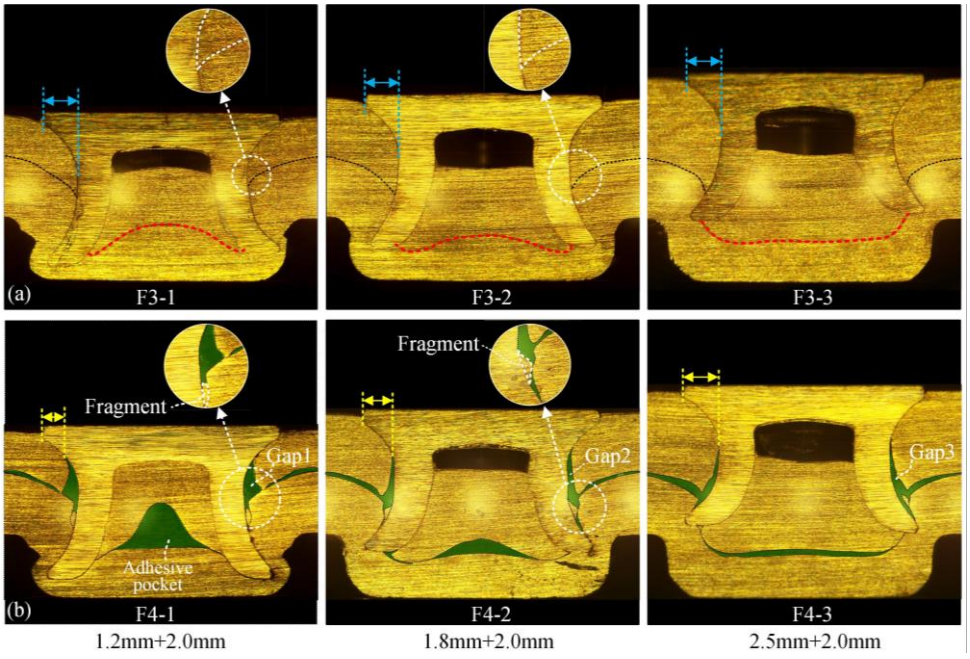

Fig. 22 Cross-sectional profiles of the SPR joints F3-1~F3-3 and the Riv-Bonded joints F4-1~F4-3 with different top sheet thicknesses T_t (Flat die)

3.2.1 Distribution of the trapped adhesive

As shown in **Fig. 21**(b), with the pip die, the T_t demonstrated a remarkable influence on the shape of the trapped adhesive pocket underneath the rivet. The 1.2mm top sheet in the joint P4-1 had relatively low rigidity and was easy to be deformed. As a result, a large amount of adhesive was accumulated around the joint central area. The 1.8mm top sheet in the joint P4-2 had a higher rigidity and became hard to be deformed. So more adhesive around the joint central area was pressed outward and a smaller amount of adhesive was trapped around the central area

compared with that in the joint P4-1. With the T_t further increasing to 2.5mm in the joint P4-3, the top sheet became much more difficult to be deformed. The bottom surface of the top sheet underneath the rivet remained almost flat during the riveting process. As a result, the adhesive was not gathered around the joint central area, but almost uniformly distributed at the interface of the two sheets. In contrast, the T_t imposed limited impact on the distribution of adhesive outside the rivet. A similar distribution pattern of adhesive was found in the Riv-Bonded joints P4-1~P4-3: only a thin adhesive layer was left between the two sheets.

As shown in **Fig. 22**(b), with the flat die, the changing trend of the trapped adhesive pocket underneath the rivet with different T_t was very similar to that in **Fig. 21**(b) with the pip die: first gathered around the joint centre with the 1.2mm top sheet in the joint F4-1 and then almost uniformly distributed between the two sheets with the 2.5mm top sheet in the joint F4-3. However, different from the Riv-Bonded joints with the pip die, the T_t also imposed a significant influence on the shape of remaining adhesive outside the rivet. Except for the thin adhesive layer left between the two sheets, there was a large amount of adhesive accumulated in the gaps (i.e. Gap 1, Gap 2 and Gap 3) around the rivet shank. As mentioned above, these gaps were formed due to the premature fracture of the top sheet and the downward displacement of the top sheet outside the rivet. The final shape and forming position of this gap were apparently affected by the T_t. With the 1.2mm top sheet in the joint F4-1, the Gap 1 had a triangle shape and was very close to the rivet head. It can be seen that the contact length between the rivet head and the top sheet (Yellow line with arrows) was obviously reduced compared with that in the joint F3-1 (Blue line with arrows). This may weaken the mechanical strengths of the riveted connection, and increase the probability of pull-out failure from the top sheet. Whilst with the 2.5mm top sheet in the joint F4-3, the Gap 3 had a strip shape and was farther away from the rivet head. Almost no influence was found on the contact length formed between the rivet head and the top sheet.

Meanwhile, it is also worth noting that, with the increment of the T_t, the reduction of the remaining adhesive in the Riv-Bonded joints might be also attributed to the changes of the initial adhesive trapped around the joining region after the clamping process. **Fig. 23** schematically shows the initially trapped adhesive after the clamping process with a thin and a thick top sheet. The thin top sheet has relatively low flexural rigidity and thus will undergo a large elastic-plastic deformation during the clamping process with a high blank-holder speed. Thus, a great amount of adhesive might be trapped around the joining region, as shown in **Fig. 23**(a). While the thick top sheet is more difficult to be deformed due to its high rigidity. Thus, more adhesive might be squeezed outside the joining region during the clamping process, and less adhesive would be trapped between the two sheets as shown in **Fig. 23**(b). The importance of die-to-rivet volume ratio for the SPR joint quality has been reported by Zhao et

al. [35], and the results revealed that a high joint quality is more likely achieved when this volume ratio is close to 1.0. After adding the adhesive layer, the trapped adhesive pocket also occupied some space of the die cavity as shown in **Fig. 21**(b) and **Fig. 22**(b). Thus, to ensure that the die cavity is large enough to accommodate all the rivet, sheets and adhesive materials, it is recommended to keep the die-to-rivet volume ratio slightly larger than 1.0 during the design of Riv-Bonded joints, especially for joints with a thin top sheet.

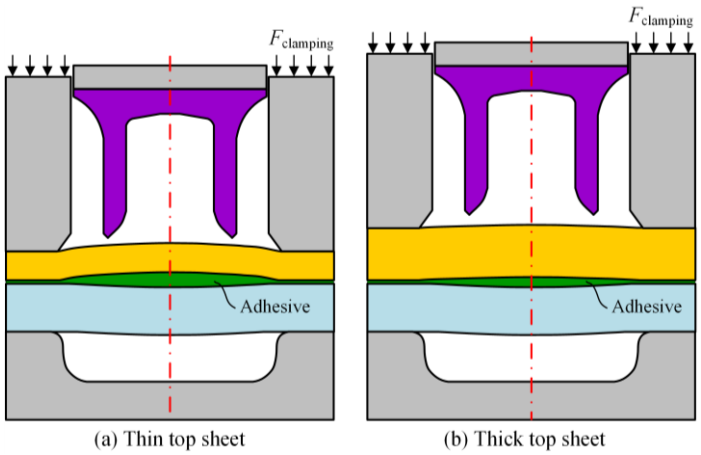

Fig. 23 Schematics of the initially trapped adhesive around the joining region after the clamping processes with (a) a thin top sheet and (b) a thick top sheet

3.2.2 Magnitude of the interlock

The magnitudes of interlock (I_1) in the SPR and the Riv-Bonded joints are shown in **Fig. 25**(a) with the pip die and in **Fig. 26**(a) with the flat die. It can be seen that, regardless of the die type, a smaller I_1 was always observed in the Riv-Bonded joints than in the corresponding SPR joints. This indicates that the adhesive layer had negative effects on the interlock formation. According to the definition, the magnitude of the I_1 is directly determined by the positions of two interlock boundaries (points *A* and *B*) shown in **Fig. 24**, and can be expressed as a function of the radiuses of interlock inner boundary (R_{in}) and outer boundary (R_{out}) in Eq.(2). To better understand the influences of the T_t and the adhesive layer on the interlock formation, the R_{in} and R_{out} in all of the twelve joints with or without the adhesive layer were also recorded in **Fig. 25**(b) with the pip die and in **Fig. 26**(b) with the flat die. It can be found that the magnitudes of the R_{in} and R_{out} were apparently influenced by the trapped adhesive. Compared with the initial values in the SPR joints, the increment amount of the R_{in} was always greater than that of the R_{out} in the Riv-Bonded joints. This directly led to the smaller I_1 in the Riv-Bonded joints than in the SPR joints.

$$I_1 = R_{out} - R_{in} \tag{2}$$

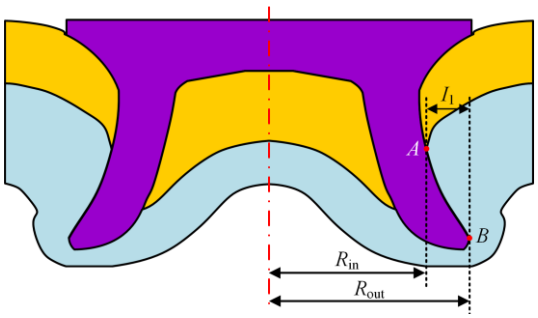

Fig. 24 Schematic of the two interlock boundaries and the corresponding boundary radiuses

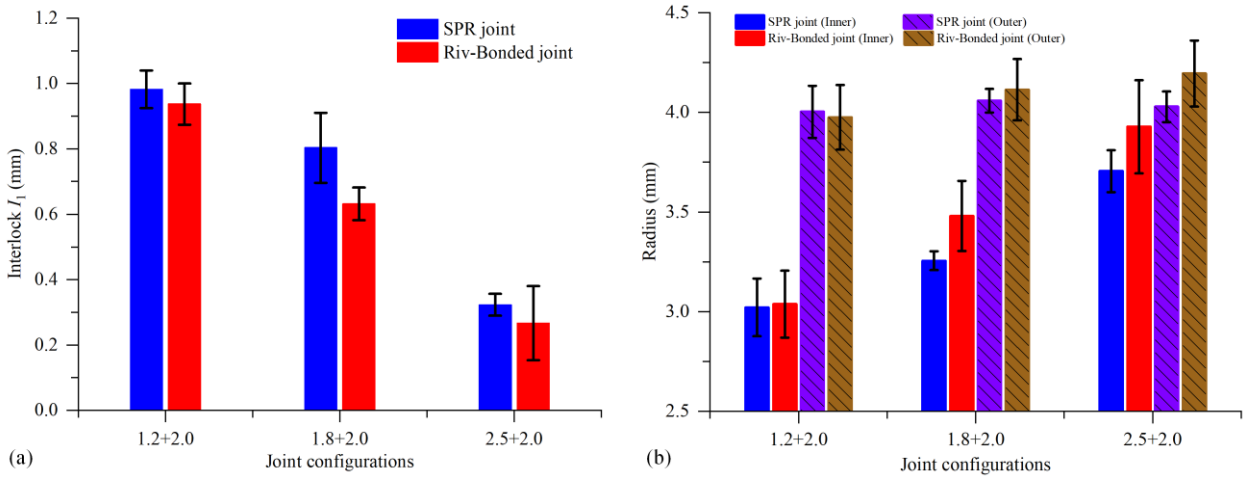

Fig. 25 Changing trends of the (a) Interlock and (b) Radius of the interlock boundaries in the SPR and Riv-Bonded joints with the Pip die

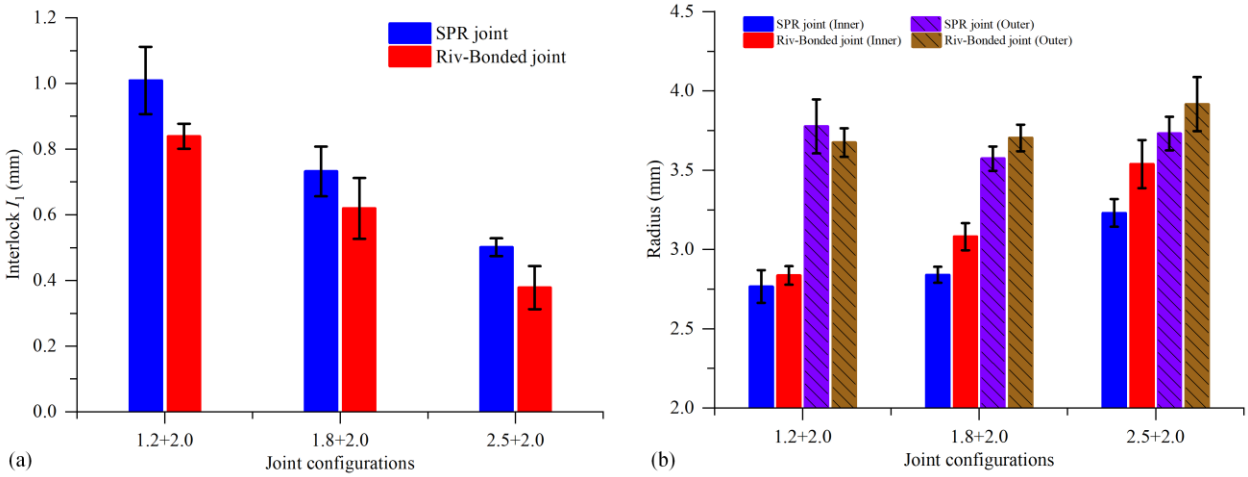

Fig. 26 Changing trends of the (a) Interlock and (b) Radius of the interlock boundaries in the SPR and Riv-Bonded joints with the flat die

In the Riv-Bonded joints with the pip die, the increased value of the R_{in} was mainly attributed to the long nose formed on the top sheet. Taking the joint P4-2 as an example, as shown in **Fig. 27**(a), a part of the nose was inserted into the interface between the rivet shank and the bottom sheet, which led to a greater outward movement of the inner interlock boundary and therefore resulted in a larger R_{in}. Similarly, in the Riv-Bonded joints with the flat die, the increment of the R_{in} was primarily caused by the top sheet fragments generated during the joining process. Taking the joint F4-2 as an example, as shown in **Fig. 27**(b), the fragment was pressed downward by the

rivet shank and finally trapped at the interface between the rivet shank and the bottom sheet. This affected the local material deformation of the bottom sheet and led to a greater R_{in}. With the different T_t, the adhesive layer showed almost the same influences on the R_{out} with the pip die and flat die. Compared with the R_{out} in the SPR joints P3-1 and F3-1, a smaller R_{out} was found in the Riv-Bonded joints P4-1 and F4-1. This is because the trapped adhesive pocket led to a larger deformation of the 1.2mm top sheet, which delayed the rivet shank flare. In contrast, compared with the R_{out} in the SPR joints P3-2, P3-3, F3-2 and F3-3, a larger R_{out} was found in the corresponding Riv-Bonded joints P4-2, P4-3, F4-2 and F4-3. This is because the 1.8mm and 2.5mm top sheets were rigid enough to avoid large deformations. The trapped adhesive pocket enhanced the guidance effects of the top sheet underneath the rivet cavity on the rivet shank flare.

Except for the impacts of the inserted nose on the interlock formation, it is also worth noting that gaps filled up with adhesive might be also formed between the rivet shank and the bottom sheet (e.g. Gap 1 in the joint P4-2 as shown in **Fig. 21**(b)). This may also weaken the mechanical performance of the riveted connection in the Riv-Bonded joints.

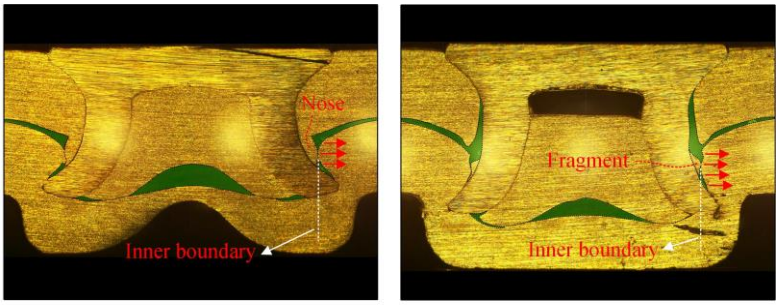

Fig. 27 Influences of (a) the nose formed with the pip die and (b) the fragment formed with the flat die on the inner interlock boundary of Riv-Bonded joints

3.2.3 Remaining bottom sheet thickness

The remaining bottom sheet thickness is very important for the corrosion performance and mechanical strengths of the SPR joints and the Riv-Bonded joints. Fatigue failure may occur on the bottom sheet if the remaining bottom sheet thickness is too small [36]. **Fig. 28** shows the magnitudes of the remaining bottom sheet thickness at the joint centre (t_c) and under the rivet tip (t_{tip}) in the SPR and the Riv-Bonded joints with 1.2mm, 1.8mm and 2.5mm top sheets. It can be seen that, with the different T_t, the adhesive layer imposed apparently different influences on the remaining bottom sheet thickness.

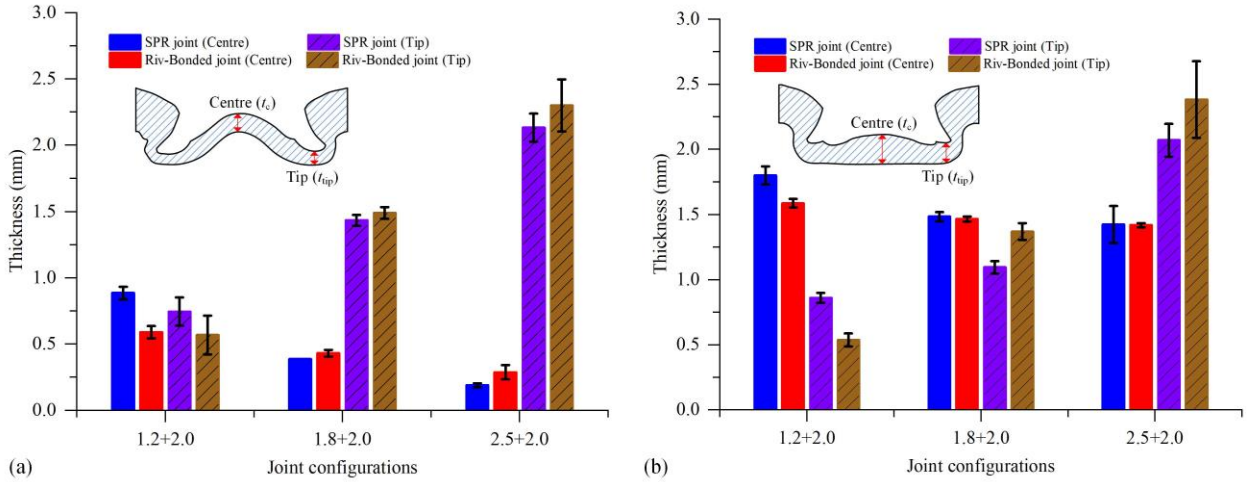

Fig. 28 Influences of the top sheet thickness T_t on the remaining bottom sheet thickness in the SPR and Riv-Bonded joints with (a) the pip die and (b) the flat die

As shown in **Fig. 28**(a), with the pip die, a smaller t_c was observed in the Riv-Bonded joint P4-1 than that in the corresponding SPR joint P3-1 with the 1.2mm top sheet. This was mainly attributed to the earlier fully filled rivet cavity in the joint P4-1 because of the trapped adhesive pocket. The rapid decrease of the t_c started again after the rivet cavity was filled up [32], and lasted for a longer period in the joint P4-1 than in the SPR joint P3-1. In contrast, with the 1.8mm and 2.5mm top sheets, a slightly larger t_c was observed in the Riv-Bonded joints P4-2 and P4-3 than in the SPR joints P3-2 and P3-3. Due to the trapped adhesive around the joint centre, the top sheet material underneath the rivet underwent a larger deformation and was bent slightly upward in the Riv-Bonded joints P4-2 and P4-3. This directly reduced the magnitude of force applied at the central area of the bottom sheet. As a result, the decreasing speed of the t_c slightly reduced in the Riv-Bonded joints compared with that in the corresponding SPR joints. Thus, the final magnitude of t_c in the Riv-Bonded joints P4-2 and P4-3 became greater than that in the SPR joints P3-2 and P3-3. As shown in **Fig. 28**(b), with the flat die, the changing trend of the t_c became slightly different. When the T_t=1.2mm, the t_c in the Riv-Bonded joint F4-1 was smaller than that in the SPR joint F3-1. This was mainly caused by the uniform hydraulic pressure applied around the central area of the bottom sheet, which changed the curved bottom sheet around the joint centre in the SPR joint F3-1 into the almost flat bottom sheet in the Riv-Bonded joint F4-1, as shown in **Fig. 22**. The trapped adhesive pocket also speeded up the filling of the rivet cavity in the joint F4-1. However, this contributed very little to the smaller t_c because the rivet cavity was fully filled almost at the end of the joining process. When the T_t=1.8mm and 2.5mm, the t_c in the Riv-Bonded joints F4-2 and F4-3 were almost the same as that in the corresponding SPR joints F3-2 and F3-3. This might be explained by the already very flat bottom sheet around the centre area of the SPR joints, and the reduction of the adhesive pocket size. The uniform hydraulic pressure in the trapped adhesive pocket imposed little influence on the bottom sheet deformation.

Regardless of the die type, the adhesive layer imposed similar influences on the bottom sheet thickness under the rivet tip (t_{tip}) in all these joints. The t_{tip} reduced to a smaller value in the Riv-Bonded joints with the 1.2mm top sheet, but obviously increased the Riv-Bonded joints with the 1.8mm and 2.5mm top sheets. This phenomenon is highly associated with the impact of the adhesive layer on the rivet shank flare behaviour (or the R_{out}), as shown in **Fig. 25**(b) and **Fig. 26**(b). A larger R_{out} usually resulted in a larger t_{tip} while a smaller R_{out} more likely led to a smaller t_{tip}.

The mechanical performance of the riveted connection is highly associated to the magnitude of interlock. From the above experimental results, the reduction of the interlock value caused by the trapped adhesive pocket would unavoidably weaken the mechanical strengths of the riveted connection. On the other hand, the trapped adhesive in the Riv-Bonded joints may also provide some benefits for the riveted connection. For instance, under the lap-shear loading condition, the top sheet underneath the rivet in the SPR joint will not provide any resistance to prevent the rivet rotation because this part of top sheet can move freely with the rivet, as shown in **Fig. 29**(a). In contrast, by adding an adhesive layer, after being cured, the adhesive accumulated around the joint centre can bond the top sheet underneath the rivet and the bottom sheet together, as shown in **Fig. 29**(b). Therefore, the top sheet inside the rivet cavity may impose a resistance on the rivet shank under the lap-shear loading condition, which might delay the rivet rotation and therefore enhance the lap-shear strength of the riveted connection in some degrees. This might explain the experimental results of lap-shear tests conducted by Miyashita et al. [2] that the riveted connection of the Riv-Bonded joint endured a greater shearing load after failure of the bonded connection than the solo SPR joint, as shown in **Fig. 30**.

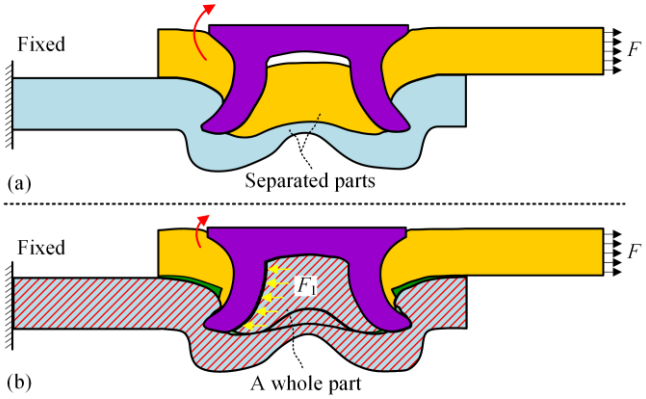

Fig. 29 Schematic of the (a) the SPR joint and (b) the Riv-Bonded joint under the lap-shear loading condition

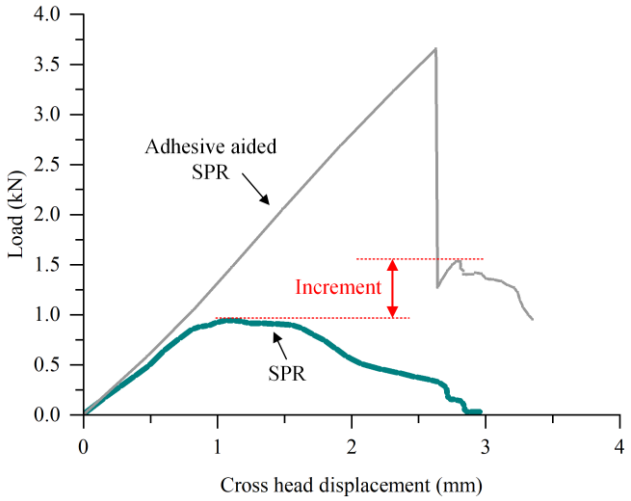

Fig. 30 Load-displacement curves during tensile shear test for SPR joint and adhesive aided SPR joint with adhesive type C [2]

4 Conclusions

In this research, influences of the adhesive layer on the events that happen during the riveting process were experimentally investigated, including the adhesive distribution, the rivet and sheets deformation behaviours and the load-displacement curve. The impacts of the trapped adhesive on the quality of joints with varying top sheet thicknesses (T_t) were analysed in detail. Two types of die (i.e. Pip die and Flat die) were utilized in the experiments to assess the possible influences of die type on the joining process as well as on the joint quality. The main conclusions are summarized below:

(1) The adhesive was distributed unevenly in the Riv-bonded joints. A large adhesive pocket was formed around the joint centre. The shape and magnitude of this adhesive pocket were significantly affected by the T_t and the clamping process, but less influenced by the die type. A thin adhesive layer was observed between the two sheets outside the rivet. A large gap filled up with the adhesive was found around the rivet shank with the flat die.

(2) The adhesive layer imposed larger influences on the top sheet deformation than on the bottom sheet deformation. In the Riv-Bonded joints, the top sheet outside the rivet underwent a smaller downward movement, but the top sheet underneath the rivet experienced a greater plastic deformation due to the trapped adhesive pocket. A long nose was formed on the top sheet when it was penetrated by the rivet shank with the pip die, but small top sheet fragments were observed with the flat die due to the premature fracture of the top sheet.

(3) The adhesive layer showed different influences on the rivet shank flare behaviour with varying T_t. Compared with sole SPR joints, the rivet shank flared a smaller distance with a small T_t, but flared a greater distance with a large T_t. The load-displacement curves were also affected by the adhesive layer, but the maximum riveting force only changed within a small range (i.e. -5kN~5kN).

(4) Compared with the corresponding SPR joints, regardless of the die types, a smaller interlock was always found in the Riv-Bonded joints. The long noses formed with the pip die and the fragments formed with the flat die directly affected the position of the left interlock boundary, and thus negatively influenced the interlock formation.

(5) The influences of adhesive layer on the remaining bottom sheet thickness varied with different T_t and die type. Compared with the corresponding SPR joints, regardless of the die types, the bottom sheet thickness at the joint centre (t_c) and under the rivet tip (t_{tip}) reduced to a smaller value in the Riv-Bonded joints with the 1.2mm top sheet. However, in the Riv-Bonded joints with 1.8mm and 2.5mm top sheets, the t_c slightly increased with the pip die but kept almost constant with the flat die. The t_{tip} achieved a larger value with both of the pip die and flat die.

All the conclusions above were made based on the employed high viscosity adhesive SikaPower 498, the specific amount of adhesive applied in the joints and the setting parameters of the SPR system. In fact, the adhesive viscosity, the adhesive amount and the speed of blank-holder will affect the joining process and the final quality of Riv-Bonded joints. Therefore, more efforts are still required in order to achieve a desired Riv-Bonded joint that can take the advantages of adhesively bonding but also maintain the original strength of riveted connection.

CRediT authorship contribution statement

Yunpeng Liu: Methodology, Writing-original draft, Writing-review & editing, Investigation. **Li Han**: Supervision, Writing-review & editing. **Huan Zhao**: Methodology, Writing-review & editing, Investigation. **Xianping Liu**: Supervision, Project administration, Funding acquisition.

Declaration of competing interest

The authors declare that they have no known competing financial interests or personal relationships that could have appeared to influence the work reported in this paper.

Data availability statement

The raw/processed data required to reproduce these findings cannot be shared at this time as the data also forms part of an ongoing study.

Acknowledgements

This work was supported by Jaguar Land Rover. The authors would like to thank Dr. Matthias Wissling, Paul Bartig and their team members from Tucker GmbH for their supports during the laboratory tests.

References

[1] G. Wu, D. Li, W.J. Lai, Y. Shi, H. Kang, Y. Peng, X. Su, Fatigue behaviors and mechanism-based life evaluation on SPR-bonded aluminum joint, Int. J. Fatigue. 142 (2021) 105948. https://doi.org/10.1016/j.ijfatigue.2020.105948.

[2] Y. Miyashita, Y.C. Jack Teow, T. Karasawa, N. Aoyagi, Y. Otsuka, Y. Mutoh, Strength of adhesive aided SPR joint for AM50 magnesium alloy sheets, Procedia Eng. 10 (2011) 2532–2537. https://doi.org/10.1016/j.proeng.2011.04.417.

[3] X. Sun, E. V. Stephens, M.A. Khaleel, Fatigue behaviors of self-piercing rivets joining similar and dissimilar sheet metals, Int. J. Fatigue. 29 (2007) 370–386. https://doi.org/10.1016/j.ijfatigue.2006.02.054.

[4] L. Lei, X. He, D. Zhao, Y. Zhang, F. Gu, A. Ball, Clinch-bonded hybrid joining for similar and dissimilar copper alloy, aluminium alloy and galvanised steel sheets, Thin-Walled Struct. 131 (2018) 393–403. https://doi.org/10.1016/J.TWS.2018.07.017.

[5] H. Jiang, C. Zeng, G. Li, J. Cui, Effect of locking mode on mechanical properties and failure behavior of CFRP/Al electromagnetic riveted joint, Compos. Struct. 257 (2021) 113162. https://doi.org/10.1016/J.COMPSTRUCT.2020.113162.

[6] F. Esmaeili, M. Zehsaz, T.N. Chakherlou, Investigation the effect of tightening torque on the fatigue strength of double lap simple bolted and hybrid (bolted-bonded) joints using volumetric method, Mater. Des. 63 (2014) 349–359. https://doi.org/10.1016/j.matdes.2014.06.021.

[7] R. Haque, J.H. Beynon, Y. Durandet, Characterisation of force–displacement curve in self-pierce riveting, Sci. Technol. Weld. Join. 17:6 (2012) 476–488. https://doi.org/10.1179/1362171812Y.0000000036.

[8] Y. Abe, T. Kato, K. Mori, Self-piercing riveting of high tensile strength steel and aluminium alloy sheets using conventional rivet and die, J. Mater. Process. Technol. 209 (2009) 3914–3922. https://doi.org/10.1016/j.jmatprotec.2008.09.007.

[9] Y. Ma, M. Lou, Y. Li, Z. Lin, Effect of rivet and die on self-piercing rivetability of AA6061-T6 and mild steel CR4 of different gauges, J. Mater. Process. Technol. 251 (2018) 282–294. https://doi.org/10.1016/J.JMATPROTEC.2017.08.020.

[10] N.H. Hoang, R. Porcaro, M. Langseth, A.G. Hanssen, Self-piercing riveting connections using aluminium rivets, Int. J. Solids Struct. 47 (2010) 427–439. https://doi.org/10.1016/j.ijsolstr.2009.10.009.

[11] H.M. Rao, J. Kang, G. Huff, K. Avery, Impact of specimen configuration on fatigue properties of self-piercing riveted aluminum to carbon fiber reinforced polymer composite, Int. J. Fatigue. 113 (2018) 11–22. https://doi.org/10.1016/J.IJFATIGUE.2018.03.031.

[12] X. Zhang, X. He, F. Gu, A. Ball, Self-piercing riveting of aluminium–lithium alloy sheet materials, J. Mater. Process. Technol. 268 (2019) 192–200. https://doi.org/10.1016/J.JMATPROTEC.2019.01.019.

[13] L. Huang, H. Guo, Y. Shi, S. Huang, X. Su, Fatigue behavior and modeling of self-piercing riveted joints in aluminum alloy 6111, Int. J. Fatigue. 100 (2017) 274–284. https://doi.org/10.1016/j.ijfatigue.2017.03.006.

[14] D. Li, A. Chrysanthou, I. Patel, G. Williams, Self-piercing riveting-a review, Int. J. Adv. Manuf. Technol. 92 (2017) 1777–1824. https://doi.org/10.1007/s00170-017-0156-x.

[15] X. He, F. Gu, A. Ball, Recent development in finite element analysis of self-piercing riveted joints, Int. J. Adv. Manuf. Technol. 58 (2012) 643–649. https://doi.org/10.1007/s00170-011-3414-3.

[16] X. Liu, Y.C. Lim, Y. Li, W. Tang, Y. Ma, Z. Feng, J. Ni, Effects of process parameters on friction self-piercing riveting of dissimilar materials, J. Mater. Process. Technol. 237 (2016) 19–30. https://doi.org/10.1016/J.JMATPROTEC.2016.05.022.

[17] H. Jiang, S. Gao, G. Li, J. Cui, Structural design of half hollow rivet for electromagnetic self-piercing riveting process of dissimilar materials, Mater. Des. 183 (2019) 108141. https://doi.org/10.1016/J.MATDES.2019.108141.

[18] H. Jiang, L. Sun, J. Liang, G. Li, J. Cui, Shear failure behavior of CFRP/Al and steel/Al electromagnetic self-piercing riveted joints subject to high-speed loading, Compos. Struct. 230 (2019) 111500. https://doi.org/10.1016/J.COMPSTRUCT.2019.111500.

[19] X. Zhang, X. He, B. Xing, W. Wei, J. Lu, Pre-holed self-piercing riveting of carbon fibre reinforced polymer laminates and commercially pure titanium sheets, J. Mater. Process. Technol. 279 (2020) 116550. https://doi.org/10.1016/J.JMATPROTEC.2019.116550.

[20] N. Baurova, A. Anoprienko, Y. Romanova, Providing dismountable rivet bonded joints through the use of hot-melt adhesives, MATEC Web Conf. 129 (2017) 01004. https://doi.org/10.1051/matecconf/201712901004.

[21] X. He, B. Xing, K. Zeng, F. Gu, A. Ball, Numerical and experimental investigations of self-piercing riveting, Int. J. Adv. Manuf. Technol. 69 (2013) 715–721. https://doi.org/10.1007/s00170-013-5072-0.

[22] Y. Liu, W. Zhuang, Self-piercing riveted-bonded hybrid joining of carbon fibre reinforced polymers and aluminium alloy sheets, Thin-Walled Struct. 144 (2019) 106340. https://doi.org/10.1016/j.tws.2019.106340.

[23] J. Presse, K. Boris, M. Thorsten, Stress-based approach for fatigue life calculation of multi-material connections hybrid joined by self-piercing rivets and adhesive, Thin-Walled Struct. 159 (2021) 107192. https://doi.org/10.1016/j.prostr.2019.12.046.

[24] H. Fricke, T. Vallée, Numerical Modeling of Hybrid-bonded Joints, J. Adhes. 92:7–9 (2016) 652–664. https://doi.org/10.1080/00218464.2015.1100995org/10.1080/00218464.2015.1100995.

[25] O. Hahn, T.M. Wibbeke, Application of low-heat hybrid joining technologies for the joining of thin-walled sheet materials, Weld. Cut. 4 (2005) 208–214.

[26] F. Moroni, Fatigue behaviour of hybrid clinch-bonded and self-piercing rivet bonded joints, J. Adhes. 95 (2019) 577–594. https://doi.org/10.1080/00218464.2018.1552586.

[27] SikaPower ® -498, 2016. https://deu.sika.com/dms/getdocument.get/741b0a84-53dc-3677-981c-e19cb4c0b6a3/SikaPower-498 DE 04-16.pdf.

[28] Y. Liu, L. Han, H. Zhao, X. Liu, Evaluation and correction of cutting position's effects on quality indicator measurement of self-piercing riveted joint, Mater. Des. (2021) 109583. https://doi.org/10.1016/J.MATDES.2021.109583.

[29] T. Gerstmann, B. Awiszus, Hybrid joining: Numerical process development of flat-clinch-bonding, J. Mater. Process. Technol. 277 (2020) 116421. https://doi.org/10.1016/j.jmatprotec.2019.116421.

[30] X. Zhang, X. He, W. Wei, J. Lu, K. Zeng, Fatigue characterization and crack propagation mechanism of self-piercing riveted joints in titanium plates, Int. J. Fatigue. 134 (2020) 105465. https://doi.org/10.1016/J.IJFATIGUE.2019.105465.

[31] X. Sun, Optimization of the strength of self-piercing rivets (SPRs), in: Self-Piercing Riveting Prop. Process. Appl., Woodhead Publishing, 2014: pp. 149–170. https://doi.org/10.1533/9780857098849.2.149.

[32] Y. Liu, H. Li, H. Zhao, X. Liu, Effects of the die parameters on the self-piercing riveting process, Int. J.

Adv. Manuf. Technol. 105 (2019) 3353–3368. https://doi.org/10.1007/s00170-019-04567-4.

[33] R. Haque, N.S. Williams, S.E. Blacket, Y. Durandet, A simple but effective model for characterizing SPR joints in steel sheet, J. Mater. Process. Technol. 223 (2015) 225–231. https://doi.org/10.1016/j.jmatprotec.2015.04.006.

[34] R. Asaro, V. Lubarda, R. Asaro, V. Lubarda, Deformation of Plates, in: Mech. Solids Mater., 2010: pp. 280–292. https://doi.org/10.1017/cbo9780511755514.017.

[35] H. Zhao, L. Han, Y. Liu, X. Liu, Modelling and interaction analysis of the self-pierce riveting process using regression analysis and FEA, Int. J. Adv. Manuf. Technol. (2021) 1–18. https://doi.org/10.1007/s00170-020-06519-9.

[36] X. Zhang, X. He, B. Xing, W. Wei, J. Lu, Quasi-static and fatigue characteristics of self-piercing riveted joints in dissimilar aluminium-lithium alloy and titanium sheets, J. Mater. Res. Technol. (2020). https://doi.org/10.1016/j.jmrt.2020.03.095.